Diffeomorphic Registration with Self-Adaptive Spatial Regularization for the Segmentation of Non-Human Primate Brains

Laurent Risser[1], Lionel Dolius[1,2], Caroline Fonta[2] and Muriel Mescam[2]

***Abstract*— Cerebral aging has been linked to structural and functional changes in the brain throughout life. Here, we study the marmoset, a small non-human primate, in order to get insights into the mechanisms of brain aging in normal and pathological conditions. Imaging the brain of small animals with techniques such as MRI, quickly becomes a challenging task when compared with human brain imaging. Very often, a simple pre-processing step such as brain extraction cannot be achieved with classical tools. In this paper, we propose a diffeomorphic registration algorithm, which makes use of learned constraints to propagate the manual segmentation of a marmoset brain template to other MR images of marmoset brains. The main methological contribution of our paper is to explore a new strategy to automatically tune the spatial regularization of the deformations. Results show that we obtain a robust segmentation of the brain, even for images with a low contrast.**

I. INTRODUCTION

The biomedical setting of this work is the study of brain aging in normal and pathological conditions, typically Alzheimer's disease. In this context, there is a growing interest in the marmoset monkey, a small non-human primate from the new world, as a model of brain aging. Indeed, besides its short life expectancy ($\sim$10 years) and low inter-subject variability (due to the small number of sulci in the cortical grey matter), the marmoset can be studied in laboratory conditions, which enables researchers to study large groups of subjects at different ages. In the last decade, neuroimaging has proven useful in relating cerebral aging to structural and functional changes in the brain throughout life [1]. More specifically, morphological modifications can generally be assessed with structural MRI. However, a number of neuroimaging applications, such as morphometric analyses or multimodal registration, necessitate prior segmentation of the brain itself from the rest of the head, or more generally of any brain structure.

Although many tools are well established to segment MR brain images acquired on humans (*e.g.*: SPM, FreeSurfer, BrainVISA, ...), no available tools are designed to segment MR brain images acquired on marmosets, to the authors knowledge. Tools available for human brains are also not adapted in this context for three main reasons: (1) Human and marmoset brain shapes are obviously different, (2) the unique available template is corrupted by a strong bias and depicts imperfections, (3) there is very little contrast between the brain and surrounding tissues in the marmoset brain MR images, as shown in Fig. 1. The driving motivation of our work is then to develop a registration algorithm sufficiently robust to propagate the manual segmentation of a marmoset brain template to other MR images of marmoset brains.

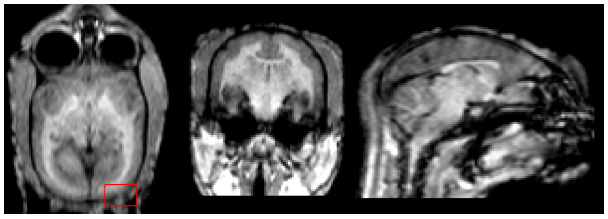

Fig. 1. 3T MRI scan of a 2-year-old marmoset (3D T1W-GRE sequence: TE = 5.2 ms, TR = 12 ms, Flip angle = 8°). The red rectangle emphasizes a region with little intensity gradients at the brain boundary.

We denote T a template image and S its segmentation (obtained manually or semi-manually). We also suppose that T is registered on image I to propagate the segmentation S on I. As the boundaries of the regions of interest in I and T are not obvious everywhere in our images, we propose in this paper a new registration algorithm which strongly constrains the deformations of T with deformations learned by registering the segmentation of T on the segmented training images I_n, $n \in [1, \cdots, N]$.

More specifically, we first perform a Principal Component Analysis (PCA) of the deformations between T and the I_n. We then constrain the deformations between T and I to be driven by the deformations resulting from the principal components of the PCA. The idea of using PCA, or Singular Value Decomposition (SVD), on deformations is not new [2]–[7]. Training sets have indeed a much lower dimension N than the number of degrees of freedom d used to encode the deformations, which requires the use of regularization techniques. These techniques also reduce d as much as possible by using spline or wavelet projection of the deformations or by subsampling the domain on which they are learned. To our knowledge, a major limitation of all existing registration approaches using an information derived from PCAs is also that the information learned strongly depends on how the deformations were spatially regularized. As seen in Fig. 2, spatial regularization has a strong influence on the deformations. The key contribution of our paper is then to explore a new strategy to make possible the automatic tuning of the spatial regularization level in diffeomorphic registration algorithm. In [8], an interesting strategy was also proposed

*This work was supported by Universite Paul Sabatier AO1 grant

[1]CNRS/Universite Toulouse 3 Paul Sabatier, Institut de Mathematiques de Toulouse (IMT UMR5219), Toulouse, France, lrisser@math.univ-toulouse.fr

[2]CNRS/Universite Toulouse 3 Paul Sabatier, Centre de Recherche Cerveau et Cognition (CERCO UMR5549), Toulouse, France, caroline.fonta and muriel.mescam@cerco.ups-tlse.fr

978-1-4244-7929-0/14/$26.00 ©2014 IEEE

to automatically control the level of spatial regularization by expanding the Free-Form-Deformations registration framework. Our approach first differs from [8] as we highly constrain our deformations to be driven by deformations learned on segmented images. Our strategy also reduces as much as possible the degrees of freedom d of the model by using *Least Absolute Shrinkage and Selection Operator* (LASSO) regularization on the model parameters. Our approach is also diffeomorphic, which ensures the estimation of one-to-one mappings without hard constraints. Note finally that spatial regularization and LASSO regularization are totally different *in practice* although mathematical relations could be established between them: spatial regularization consists in smoothing a vector field encoding the deformations between two registered images while LASSO regularization consists in penalizing a norm between the model parameters encoded in a single vector.

In section II, we give a general overview of the LogDemons algorithm [9] that we use to learn reference velocity fields and then describe our registration algorithm. General segmentation pipeline, data treatment, and results are then given in section III.

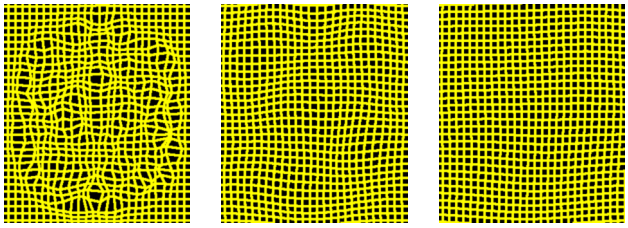

$\sigma = 0.5$mm $\quad$ $\sigma = 3$mm $\quad$ $\sigma = 7$mm

Fig. 2. Displacement fields obtained after registering a brain template image T on another brain image I using LogDemons registration [9] with three levels of fluid regularization: Gaussian kernels of standard deviation σ equals to 0.5, 3 or 7 mm.

II. METHODOLOGY

A. Overview of the Log-Demons Formalism

In this subsection, we give an overview of the Log-Demons registration algorithm [9], as we use it to learn typical deformations between the template image T and other images I. Suppose that T and I are affinely aligned. Image T is transformed through the diffeomorphic transformation $\phi_{\mathbf{t}}$, $t \in [0,1]$ which is defined by a stationary velocity field $\mathbf{v} \in \Omega$ using:

$$\frac{\partial}{\partial_t}\phi_{\mathbf{t}} = \mathbf{v}(\phi_{\mathbf{t}})\,, \tag{1}$$

where $\phi_{\mathbf{0}} = \mathbf{Id}$. This integration can be quickly performed using the method of [10]. Deformed template image is then $T \circ \phi_{\mathbf{1}}$. Optimal velocity field $\mathbf{v}$ is obtained by minimizing an energy which maximizes the sum of squared differences (SSD) between the registered images for sufficiently smooth deformations. *Update velocity field* is defined as:

$$\delta(\mathbf{x}) = -\frac{I - T \circ \phi_{\mathbf{1}}}{||\mathbf{J}(\mathbf{x})||^2 + \lambda_i^2/\lambda_x^2}\mathbf{J}(\mathbf{x})\,, \tag{2}$$

where $\mathbf{J}(\mathbf{x}) = \nabla(T \circ \phi_{\mathbf{1}})(\mathbf{x})$, $\mathbf{x} \in \Omega$ denotes the intensity gradients. Registration is performed using Alg. 1 where the Baker-Campbell-Hausdorff (BCH) formula is: $\mathbf{v_c} \simeq \mathbf{v} + \delta + [\mathbf{v}, \delta]/2$, and the Lie bracket is defined by $[\mathbf{v_1}, \mathbf{v_2}] = (\nabla \mathbf{v_1})\mathbf{v_2} - (\nabla \mathbf{v_2})\mathbf{v_1}$. We denote Γ the parameters which control the *spatial regularization* of $\mathbf{v}$. In particular, Γ contains the standard deviations of the Gaussian kernels used to perform fluid and diffusion regularization. Insights about these parameters are given in [11].

Alg. 1 Overview of the registration algorithm [9]

Require: Template T, target I, parameters Γ
1: Initialize $\mathbf{v}$ as null
2: **while** Not convergence of $\mathbf{v}$ **do**
3: Compute $\phi_{\mathbf{1}}$ using Eq. (1)
4: Compute the update velocity field δ using Eq. (2).
5: **Fluid regularization**: Gaussian smoothing of δ.
6: Estimate $\mathbf{v_c} = BCH(\mathbf{v}, \delta)$, where $BCH(.,.)$ is the Baker-Campbell-Hausdorff formula.
7: **Diffusion regularization**: Update $\mathbf{v}$ by smoothing $\mathbf{v_c}$ with a Gaussian kernel.
8: **end while**

B. Highly-constrained diffeomorphic registration

Our algorithm is inspired from [9] but we use a totally different technique to regularize the velocity field $\mathbf{v}$. Deformations are now strongly constrained by constructing $\mathbf{v}$ as the weighted sum of K reference velocity fields $\mathbf{v_k}$:

$$\mathbf{v} = \sum_{k=1}^{K} \alpha_k \mathbf{v_k}\,, \tag{3}$$

where the weights α_k are the parameters to estimate. We denote Θ these parameters. A first version of our algorithm is given in Alg. 2, where $\cdot$ denotes the dot product between two vectors and ϵ controls the updates scale.

Alg. 2 Registration algorithm without regularization of Θ

Require: Template T, target I, reference velocity fields $\mathbf{v_k}$
1: Initiate $\alpha_k = 0$, $\forall k \in \{1, \cdots, K\}$
2: **for** Iteration $\in [1, \cdots, N]$ **do**
3: Compute $\phi_{\mathbf{1}}$ using Eq. (1)
4: Compute the update velocity field δ using Eq. (2)
5: **for** $k \in \{1, \cdots, K\}$ **do**
6: $\tilde{\alpha_k} = \sum_{x \in \Omega} \mathbf{v_k}(x) \cdot \delta(x)$
7: $\alpha_k = \alpha_k + \epsilon \tilde{\alpha_k}$
8: **end for**
9: Reconstruct $\mathbf{v}$ using Eq. (3)
10: **end for**

C. Registration with self-adaptive regularization level

Note that the algorithm of section II-B is not well posed, as no constraint was given to regularize the weights $\Theta = \{\alpha_1, \cdots, \alpha_K\}$. This algorithm is then likely to diverge. We use *Least Absolute Shrinkage and Selection Operator* (LASSO) regularization on the weights of Θ, which allows to address a self-adaptive spatial regularization of $\mathbf{v}$ using the technique explained hereafter.

1) Learning step: The first key of our strategy is to learn the reference velocities $\mathbf{v_k}$ using different spatial regularization parameters Γ in Alg. 1. We consider r sets of parameters Γ. For instance, we can define Gaussian kernels with r different standard deviations to perform fluid regularization in Alg. 1. We also denote I_n, $n \in [1, \cdots, N]$ the set of training images. For a given set of parameters Γ, we register the template T on all training images I_n using Alg. 1. We then obtain N velocity fields $\mathbf{v_n}$, $n \in [1, \cdots, N]$. A PCA is performed on these fields and we keep the c first components of the PCA, where c is typically equal to $\{1, 2, 3\}$ (see Fig. 3). By repeating this process for each set of parameters Γ, we obtain the $K = rc$ reference velocities $\mathbf{v_k}$. Note that if T is not the average of the I_n, it is important to use the average deformation in addition to the principal components.

2) Registration: Our registration algorithm is the same as the one of section II-B, except that we perform LASSO regularisation on Θ, *i.e.* we penalize $\beta||\Theta||_1 = \beta(\sum_{k=1}^{K} |\alpha_k|)$. This is the second key of our strategy. LASSO regularization is well known in statistics to set to zero the parameters which have little influence on what a model explains. In our context, it will set to zero the values α_k associated to vectors $\mathbf{v_k}$ which are the least pertinent to represent the optimal deformation. Only the most pertinent velocity fields $\mathbf{v_k}$ will then contribute to $\mathbf{v}$ in Eq. (3). Note that the higher β, the stronger this property. As the different $\mathbf{v_k}$ represent velocity fields obtained using different levels of spatial regularization, this property is automatically tuned here. In practice, this regularization is performed using the derivative of $\beta||\Theta||_1$ relative of each term α_k, which is equal to $(\beta\alpha_k)/|\alpha_k|$. In line 7 of Alg. 2, we then replace $\alpha_k = \alpha_k + \epsilon\tilde{\alpha_k}$ with:

$$\alpha_k = \alpha_k + \epsilon \left(\tilde{\alpha_k} - \frac{\beta \alpha_k}{|\alpha_k|} \right) . \quad (4)$$

The derivative is not defined for $\alpha_k = 0$. If the sign of α_k is changed during Eq. (4), we then simply set α_k to 0.

III. RESULTS

A. Material and experimental protocol

Eleven T1-weighted images were acquired in adult marmosets using a 3D gradient echo sequence (parameters: TE = 5.2 ms, TR = 12 ms, Flip angle = 8°) on a 3T MRI Philips scanner[1]. The resulting images have a resolution of about 0.4 mm (see Fig. 1). Manual segmentation of the brain was performed on a set of eight images using Matlab® to serve as a basis for the learning step, whereas the three remaining images were used to test the algorithm.

B. Learning step

We picked-up one of the segmented images as the template T and considered the 7 remaining ones as the learning set of images I_n. Affine alignment of all images on T was first performed using ANTS[2]. Template T was then registered on the I_n, $n \in [1, \cdots, 7]$ using [9] with $r = 6$ sets of parameters Γ. More specifically, we used $r = 6$ different standard deviations $\sigma = \{0.5, 1, 2, 3, 5, 7\}$mm for the Gaussian kernel used to perform fluid regularization. Very little diffusion regularization was performed as we used a Gaussian kernel with a standard deviation equals to 0.1mm. Image registration algorithm was coded in C++ with openMP parallelization. PCA of the velocity fields obtained using each parameters set Γ was performed in Python using the scikit-learn library. We kept the 3 principal components of each PCA (see Fig. 3). As T is not the average of the training images, we also used the average deformation. In the end, we have $K = 4 * 7$ reference velocity fields $\mathbf{v_k}$.

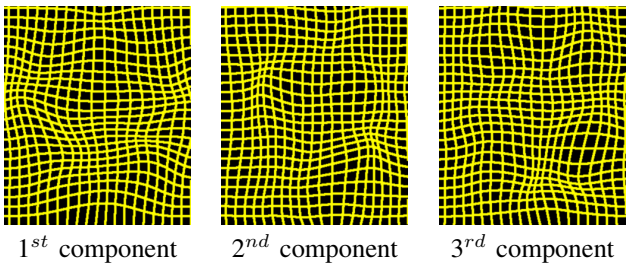

Fig. 3. Displacement fields obtained using the PCA of the velocity fields $\mathbf{v_n}$ learned with the fluid regularization kernel σ = 2mm. Three first components of the PCA are shown.

C. Registration of the template and segmentation

After learning K reference velocity fields $\mathbf{v_k}$ obtained using different levels of spatial regularization, we registered T on 3 test images with the registration technique of section II-C. We denote L-LD$_\beta$ this technique, where β is the value given to the LASSO regularization parameter. We also compared the proposed strategy with [9] using Gaussian kernels with σ = 0.5mm and σ = 2mm to perform fluid regularization. We denote LD$_\sigma$ this technique. LD$_\sigma$ obviously leads to far less constrained deformations than L-LD$_\beta$. Deformations are therefore more flexible to match image details but are subject to implausible deformations if intensity gradients do not properly represent brain boundaries.
As shown in Fig. 4, brain boundaries were always properly found, even for Image 1 (shown Fig. 1) which has locally low intensity gradients at the brain boundaries.

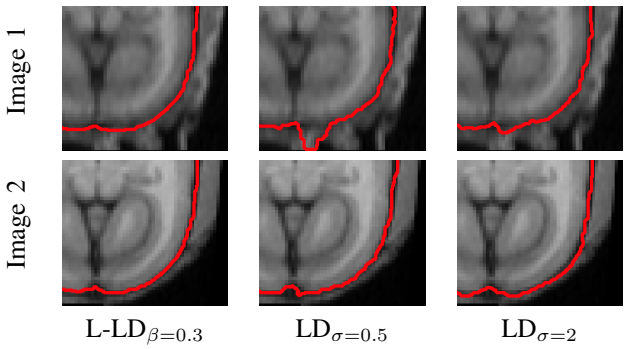

Fig. 4. Propagation of the brain mask after registering the template T on two test images I using our method (L-LD) and [9] (LD) with a fluid regularisation σ equals to 0.5mm or 2mm. Results are shown in an ROI of images 1 and 2 with little intensity gradients at the brain boundary. The red isoline represents the estimated brain boundary.

[1]This study was approved by the French Regional Committee for the use of laboratory animals (authorization # MP/03/76/11/12).

[2]http://stnava.github.io/ANTs/

We also measured the sum of square differences (SSD) between the registered images in the brain (normalized by the SSD before registration) as well as the maximum determinant of the deformation Jacobians (max DetJ) to quantify the matching quality and the deformation smoothness. Average SSD obtained using $\text{LD}_{\sigma=0.5}$ and $\text{LD}_{\sigma=2}$ were 0.25 and 0.60, respectively. Corresponding Max DetJ were also 49 and 7.79, respectively. Results obtained for different values of β are shown in Table I. We can first observe that LD_{σ} gave better matchings than L-LD_{β} as it is more flexible, as also shown by the higher Max DetJ. The Max DetJ obtained using $\text{LD}_{\sigma=0.5}$ is particularly high which emphasizes physiologically implausible deformations. Deformations of $\text{LD}_{\sigma=2}$ seem more realistic. It is worth noticing that L-$\text{LD}_{\beta=1}$ however led to an almost similar matching quality than $\text{LD}_{\sigma=2}$ for much smoother deformations, which is an encouraging result. We finally assessed the influence of β on the results. Interestingly, the best results between matching quality and deformation smoothness were not obtained with the larger amount of weights $\alpha_k > 0$, but using only 29% of the $\alpha_k > 0$ (for β =1). Note also that for the three different images on which T was registered, the $\mathbf{v_k}$ related to the highest α_k were obtained using different levels of spatial regularization. This seems to show that our self-adaptive regularization technique makes sense here.

TABLE I

AVERAGE RESULTS OBTAINED USING L-LD_{β}.

	$\beta = 0.1$	$\beta = 0.3$	$\beta = 1$	$\beta = 2$
Max DetJ	4.16	2.31	1.72	1.30
SSD	0.81	0.79	0.70	0.81
% ($\alpha_k > 0$)	89	59	29	12

IV. DISCUSSION

From these results, we conclude that by strongly constraining the deformations, we are able to perform a robust segmentation of the brain, even for images with a low contrast. Interestingly, we obtain the best compromises between image matching and deformation smoothness using sparse mixtures of deformations with smoothness levels depending on the registered image.

Considering that extracting the brain from its surrounding tissues is a crucial step towards more advanced image processing and analysis, this method widens the possibilities for further analysis. Indeed, we now expect to be able to reliably quantify changes in small animals, such as marmosets, and with clinical devices instead of dedicated but also costly high-resolution devices. More generally, our algorithm should prove useful for the segmentation of any structure in poorly contrasted brain regions. In addition, gaining knowledge on the mechanisms involved in normal and pathological aging of the brain, requires longitudinal analyses on large sets of data. In this context, it is important to provide a processing pipeline that is the most automatic possible.

On a methological side, there are different perspectives to make our registration strategy more efficient. First, defining the template as the average of the training images would reduce the number of reference fields as the average deformation would be almost zero. In addition, learning reference deformations using image- and landmark-based registration could also help capture more realistic deformations if we want to segment all brain structures and not only the brain boundary. Furthermore, allowing multimodal registration, by maximizing the mutual information for instance, would also be an interesting feature to add to our strategy. Indeed, combining modalities such as CT, SPECT, or PET, with structural MRI, would definitely help not only localizing, but also linking both morphological and functional (*e.g.* perfusion, metabolism) modifications occurring in the brain throughout life.

From a research perspective in image registration, we finally believe that defining learning strategies with finer models, in particular which take into account the deformations location, would be of high interest. Assessing whether regularization strategies other than LASSO would lead to better results is also foreseen.

ACKNOWLEDGMENT

We acknowledge the CerCo animal rearing facilities, the MRI platform of the Institute of Brain Sciences of Toulouse, and Nathalie Vayssiere for her help with MRI acquisition.

REFERENCES

[1] A. M. Fjell, L. T. Westleye, H. Grydeland, I. Amlien, T. Espeseth, I. Reinvang, N. Raz, A. M. Dale and K. B. Walhovd, "Accelerating cortical thinning: unique to dementia or universal in aging?," *Cerebral Cortex*, vol. 24, pp. 919–34, 2014.

[2] D. Rueckert, A. Frangi, and J. A. Schnabel, "Automatic construction of 3D statistical deformation models of the brain using nonrigid registration," *IEEE Transactions on Medical Imaging*, vol. 22, no. 3, pp. 1014–25, 2003.

[3] Z. Xue, D. Shen, and C. Davatzikos, "Statistical representation of high-dimensional deformation fields with application to statistically constrained 3D warping," *Medical Image Analysis*, vol. 10, no. 5, pp. 740–51, 2006.

[4] T. He, Z. Xue, W. Xie, and S. T. C. Wong, "Online 4D CT estimation for patient-specific respiratory motion based on real-time breathing signals," in *Proc. MICCAI*, 2010, p. 392-99.

[5] M. J. Kim, M. H. Kim, and D. Shen, "Learning-based deformation estimation for fast non-rigid registration," in *Proc. CVPRw*, 2008, pp. 1–6.

[6] J. A. Onofrey, L. H. Staib, and X. Papademetris, "Learning nonrigid deformations for constrained multi-modal image registration," in *Proc. MICCAI*, 2013, pp. 171–8.

[7] N. Singh, P. T. Fletcher, J. S. Preston, R. D. King, J. S. Marron, M. W. Weiner, and S. Joshi, "Quantifying anatomical shape variations in neurological disorders," *Medical Image Analysis*, In press, 2014.

[8] I. J. A. Simpson, M. W. Woolrich, M. J. Cardoso, D. M. Cash, M. Modat, J. A. Schnabel, and S. Ourselin, "A bayesian approach for spatially adaptive regularisation in non-rigid registration," in *proc. MICCAI*, 2013, pp. 10–18.

[9] T. Vercauteren, X. Pennec, A. Perchant, and N. Ayache, "Symmetric log-domain diffeomorphic registration: A demons-based approach," in *Proc. MICCAI*, 2008, pp. 754–761.

[10] V. Arsigny, O. Commowick, X. Pennec, and N. Ayache, "A log-Euclidean framework for statistics on diffeomorphisms," in *Proc. MICCAI*, 2006, number 4190, pp. 924–931.

[11] T. Mansi, X. Pennec, M. Sermesant, H. Delingette, and N. Ayache, "iLogDemons: A demons-based registration algorithm for tracking incompressible elastic biological tissues," *IJCV*, vol. 92, no. 1, pp. 92–111, 2011.